Published by IOP Publishing for SISSA

Received: *September 21, 2009*
Accepted: *September 25, 2009*
Published: *October 19, 2009*

Bound-state effects on gluino-pair production at hadron colliders

Kaoru Hagiwara[a] **and Hiroshi Yokoya**[b]

[a] *KEK Theory Center and Sokendai, Tsukuba 305-0801, Japan*
[b] *Theory Unit, Physics Department, CERN, CH-1211 Geneva, Switzerland*

E-mail: hiroshi.yokoya@cern.ch

Abstract: We study bound-state effects on the pair production of gluinos at hadron colliders, in a context of the minimal supersymmetric extension of the standard model. Due to the expected large mass and the octet color-charge of gluinos, the bound-state effects can be substantial at the LHC. We find significant deformation of the invariant-mass distributions of a gluino-pair near the mass threshold, as well as an additional correction to the total cross-section. Both the invariant-mass distribution and the correction to the total cross section depend crucially on the decay width of the gluino.

Keywords: Supersymmetric Standard Model, Hadronic Colliders, QCD

ArXiv ePrint: 0909.3204

doi:10.1088/1126-6708/2009/10/049

JHEP10(2009)049

Contents

1 Introduction **1**

2 Gluino decay-width **2**

3 Gluino-pair production cross-section **4**
3.1 $gg \to \tilde{g}\tilde{g}$ process 4
3.2 $q\bar{q} \to \tilde{g}\tilde{g}$ process 6

4 Binding corrections **7**

5 ISR corrections **11**

6 Summary **13**

1 Introduction

At the CERN Large Hadron Collider (LHC), discovery of new heavy particles at TeV scale is expected as an evidence of physics beyond the Standard Model (SM). One of the well-investigated models beyond the SM is the minimal supersymmetric extension of the Standard Model (MSSM). At hadron colliders, colored particles can be produced copiously. In the MSSM, the colored particles are superpartners of quarks and gluons, which are called squarks and gluinos, respectively. The LHC has high discovery potential for those particles, where masses up to 2 TeV can be explored [1, 2]. Current limits on their mass and production cross-sections are set by measurements at the Fermilab Tevatron collider [3, 4] (See also ref. [5]).

In the MSSM, due to the R-parity conservation, superpartner particles or sparticles, are produced in pair. The total and differential cross-sections at hadron colliders have been known for long time in the leading-order (LO) [6–8], as well as in the next-to-leading oder (NLO) including SUSY-QCD corrections [9–11]. The NLO corrections are found to positive and large. The origin of the large corrections comes from the threshold logs due to the emission of the soft/collinear gluons, and also a Coulomb singularity due to the exchange of Coulomb gluons between the final-state particles. Both terms become significant at the partonic threshold region, where they should be considered to all-order. Recently, the all-order summation of the threshold logarithmic corrections has been performed for the sparticle-pair production processes at hadron colliders in refs. [12–14].

The aim of this paper is to examine the effects of Coulomb corrections to all-orders in the gluino-pair production process. Similar studies for gluino-pair and also squark-pair productions can be found in ref. [14], where the Coulomb corrections are taken into account

JHEP10(2009)049

to all-orders by using the Sommerfeld factor [15, 16]. However, to our knowledge, there has been no study including the bound-states effect which have been found significant for the top-quark pair production at the LHC [15, 17, 18].[1] The bound-states of a pair of gluinos are called *gluinonium* [20–28]. When the Coulomb force is attractive, it causes not only the corrections to the cross-sections above the mass threshold [14], but also formation of the gluinoniums below the threshold. The bound-state formations can be taken into account by summing the Coulomb terms to all-orders or non-perturbatively. The Green's function formalism [29, 30] has been developed for this purpose, which incorporates the finite-width effects of the constituent particles.

The paper follows the recent studies for the bound-state effects in the top-quark pair production at hadron colliders [17, 18]. The invariant-mass distribution of the top-quark pair is distorted significantly near the threshold region [17, 18], and we may expect similar effects for the gluino-pair.

The paper is organized as follows: in section 2 and section 3, we briefly review the basic properties of the gluino decay-width and the gluino-pair production cross-section, respectively. Then in section 4, we discuss binding corrections to the gluino-pair production. In section 5, we discuss effects of the initial-state radiation and the hard-vertex correction. Finally, we summarize our findings in section 6.

2 Gluino decay-width

In this section and the next section, we briefly review the basic properties of the gluino that are relevant to our studying; the decay-width and the pair-production cross-section at hadron colliders, respectively. For more details, see e.g. ref. [31].

The effects of gluinonium formation at hadron colliders depend strongly on the gluino decay width. In particular, the following regions should have qualitatively different signals:

$$A: \quad \Gamma_{\tilde{g}} \gtrsim |E_B| \tag{2.1a}$$

$$B: \quad |E_B| > \Gamma_{\tilde{g}} \gg \Gamma_{gg} \tag{2.1b}$$

$$C: \quad |E_B| \gg \Gamma_{\tilde{g}} > \Gamma_{gg} \tag{2.1c}$$

$$D: \quad \Gamma_{\tilde{g}} < \Gamma_{gg} \tag{2.1d}$$

Here, $E_B < 0$ is the binding-energy of gluinoniums, and Γ_{gg} denotes the partial decay-width of the gluinonium annihilation into gluons. In the region A, the produced gluinos decay before the gluinonium formation, and the binding effects cannot be observed. In the region B, the binding effects are expected to enhance the pair production cross-section below the threshold, especially at around the location of the ground state energy, as is expected for the top-quarks [15, 17, 18]. In the region C, a few narrow gluinonium resonances can be produced, whose decay may still be dominated by the constituent gluino decays. In the region D, the produced gluinonium will decay mainly into gluon jets, and hence will disappear without leaving a detectable trace in hadron collider environments.

[1] We are informed that the bound-state effect on the squark pair production is examined in ref. [19].

JHEP10(2009)049

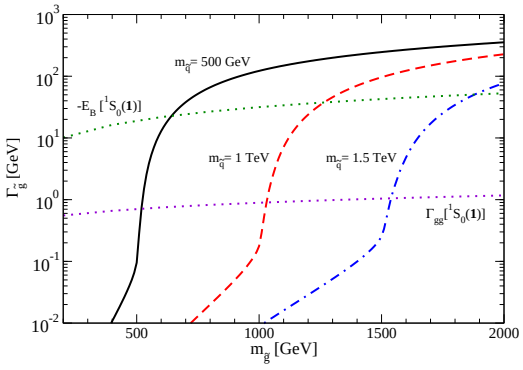

Figure 1. The gluino decay-width as a function of the gluino mass, calculated from $\tilde{g} \to q\bar{q}^{(\prime)}\tilde{W}$ and $\tilde{g} \to q\bar{q}\tilde{B}$ decay modes. We consider decays into 5-flavor massless quarks only where the corresponding squarks have a common mass $m_{\tilde{q}} = 500\,\text{GeV}$, 1 TeV or 1.5 TeV, and the gaugino masses satisfy $m_{\tilde{g}} : m_{\tilde{W}} : m_{\tilde{B}} = 7 : 2 : 1$. The dotted-lines show the magnitude of the binding energy of the ground $^1S_0(\mathbf{1})$ gluinonium ($-E_B[^1S_0]$), and the partial decay-width of the ground $^1S_0(\mathbf{1})$ gluinonium annihilation into gluons ($\Gamma_{gg}[^1S_0]$).

In figure 1, we plot the decay width of the gluino as a function of the gluino mass. The decay-width is calculated for $\tilde{g} \to q\bar{q}^{(\prime)}\tilde{W}$ and $\tilde{g} \to q\bar{q}\tilde{B}$ decays [32], where winos ($\tilde{W}$) and a bino ($\tilde{B}$) are superpartners of SU(2)_L and U(1)_Y gauge bosons, respectively. Solid, dashed and dot-dashed curves are for the squark mass $m_{\tilde{q}} = 500\,\text{GeV}$, 1 TeV and 1.5 TeV, respectively. For simplicity, we assume that all the super-partners of 5 light-quarks with both chiralities have a common mass $m_{\tilde{q}}$, and the gaugino masses satisfy the relation $m_{\tilde{g}} : m_{\tilde{W}} : m_{\tilde{B}} = 7 : 2 : 1$, which are valid in several SUSY breaking scenarios. Neither the contribution from the top squarks nor the gaugino-higgsino mixing are considered for brevity.

The upper dotted-line shows the magnitude of the binding energy of the ground $^1S_0(\mathbf{1})$ gluinonium, which is the most deeply-bounded color-singlet gluinonium, see section 4 in detail. It is estimated by using a Coulombic potential $V(r) = -C_A\alpha_s/r$ with the color-factor $C_A = 3$ for the color-singlet gluinoniums. Within this approximation, the binding-energy is calculated as

$$E_B[^1S_0(\mathbf{1})] = -\frac{C_A^2}{4} m_{\tilde{g}} \alpha_s^2(\mu_B)_{\overline{\text{MS}}}, \tag{2.2}$$

where we take the $\overline{\text{MS}}$ renormalization scale to satisfy $\mu_B = C_A m_{\tilde{g}} \alpha_s(\mu_B)_{\overline{\text{MS}}}/4$, which corresponds to a half of the inverse Bohr radius of the $^1S_0(\mathbf{1})$ gluinonium. It is known that this scale choice makes the QCD higher-order corrections to the binding energy small. For the gluino-mass from 200 GeV to 2 TeV, the binding energy grows from $\sim 10\,\text{GeV}$ to $\sim 50\,\text{GeV}$.

The lower dotted-line shows the partial decay-width of the ground $^1S_0(\mathbf{1})$ gluinonium annihilation into two gluons;

$$\Gamma_{gg}[^1S_0(\mathbf{1})] = 18\pi\alpha_s^2 \left(\frac{m_{\tilde{g}}}{2}\right)_{\overline{\text{MS}}} \cdot \frac{|\psi(0)|^2}{m_{\tilde{g}}^2}, \tag{2.3}$$

with $|\psi(0)|^2 = C_A^3 m_{\tilde{g}}^3 \alpha_s^3(\mu_B)_{\overline{\text{MS}}}/8\pi$ which is also obtained by using the Coulombic potential approximation. For the same gluino-mass region as above, it grows from several hundred MeM to one GeV.

JHEP10(2009)049

Figure 2. Feynman diagrams for $gg \to \tilde{g}\tilde{g}$ process and $q\bar{q} \to \tilde{g}\tilde{g}$ process at the tree-level. Dashed-lines represent squarks, $\tilde{q}_R$ or $\tilde{q}_L$.

The three curves for $\Gamma_{\tilde{g}}$ show steep gradient at $m_{\tilde{g}} \simeq m_{\tilde{q}}$. Above the squark mass threshold, the gluinos decay into a squark and a quark and the width is proportional to $\alpha_s m_{\tilde{g}}$. Below the two-body decay threshold, the gluino decay width drops quickly down to the three-body decay width with the electroweak coupling. The gluino width curves cross the binding-energy curve at around $m_{\tilde{g}} \simeq 1.3 m_{\tilde{q}}$, while they cross the gluinonium annihilation width just above $m_{\tilde{g}} = m_{\tilde{q}}$. Therefore, if the gluino is lighter than all the squarks, the region D (2.1d) would likely be realized, and binding effects cannot be observed at hadron colliders. On the other hand for $m_{\tilde{g}} > m_{\tilde{q}}$, depending on the mass ratio $m_{\tilde{g}}/m_{\tilde{q}}$, regions A to C (2.1a-c) would be realized.

3 Gluino-pair production cross-section

Now, we review the gluino-pair production at hadron colliders, focusing our attention on the threshold behavior and the color structure of the scattering amplitudes.

At the parton level, there are two leading subprocesses for the gluino-pair production;

$$g(p_1, \lambda_1, a_1) + g(p_2, \lambda_2, a_2) \to \tilde{g}(p_3, \lambda_3, a_3) + \tilde{g}(p_4, \lambda_4, a_4), \tag{3.1a}$$

$$q(p_1, \lambda_1, i_1) + \bar{q}(p_2, \lambda_2, i_2) \to \tilde{g}(p_3, \lambda_3, a_3) + \tilde{g}(p_4, \lambda_4, a_4). \tag{3.1b}$$

The tree-level Feynman-diagrams are shown in figure 2. Here, p_k and λ_k are momenta and helicities of particles, a_k and i_k are color indices of gluons(gluinos) and quarks, respectively. We normalize λ_k to take ± 1 both for fermions and gluons. At the LHC, due to the steep rise of the gluon density in the small momentum-fraction region, gluon-fusion process (3.1a) dominates the cross section for $m_{\tilde{g}} < 1\,\mathrm{TeV}$ [9]. For $m_{\tilde{g}} > 1\,\mathrm{TeV}$, the $q\bar{q}$ annihilation process (3.1b) can contribute significantly to the total cross-section.

3.1 $gg \to \tilde{g}\tilde{g}$ process

First, we review the gluon-fusion process. We present helicity amplitudes for this process by decomposing the color factors into symmetric and antisymmetric parts:

$$\mathcal{M}_{gg\to\tilde{g}\tilde{g}}(p_i; \lambda_i; a_i) = g_s^2 \left[\frac{1}{2} \left\{ F^{a_3}, F^{a_4} \right\}_{a_1 a_2} M_{gg}(p_i; \lambda_i) + \frac{1}{2} \left[F^{a_3}, F^{a_4} \right]_{a_1 a_2} N_{gg}(p_i; \lambda_i) \right]. \tag{3.2}$$

Here $g_s = \sqrt{4\pi\alpha_s}$ is the QCD coupling constant. $F^a_{bc} = -if^{abc}$ is the color matrix in the adjoint representation. The amplitudes can be obtained by replacing only the color-factors from those of the heavy-quark pair production, $gg \to Q\bar{Q}$. The color-symmetric part and

JHEP10(2009)049

antisymmetric part of the amplitudes are summarized as follows;

$$M_{gg}(p_k;\lambda,\lambda,\bar{\lambda},\bar{\lambda}) = \frac{4m_{\tilde{g}}}{\sqrt{\hat{s}}}\frac{\lambda+\bar{\lambda}\beta}{1-\beta^2\cos^2\theta}, \tag{3.3a}$$

$$M_{gg}(p_k;\lambda,\lambda,\bar{\lambda},-\bar{\lambda}) = 0, \tag{3.3b}$$

$$M_{gg}(p_k;\lambda,-\lambda,\bar{\lambda},\bar{\lambda}) = -\bar{\lambda}\frac{4m_{\tilde{g}}}{\sqrt{\hat{s}}}\frac{\beta\sin^2\theta}{1-\beta^2\cos^2\theta}, \tag{3.3c}$$

$$M_{gg}(p_k;\lambda,-\lambda,\bar{\lambda},-\bar{\lambda}) = -2\frac{\beta\sin\theta(\lambda\bar{\lambda}+\cos\theta)}{1-\beta^2\cos^2\theta}, \tag{3.3d}$$

for the symmetric part, and

$$N_{gg}(p_k;\lambda_k) = \beta\cos\theta\cdot M_{gg}(p_k;\lambda_k). \tag{3.4}$$

for the anti-symmetric part. Here, θ is the angle between the 3-momenta $\vec{p}_1$ and $\vec{p}_3$, and $\beta = \sqrt{1-4m_{\tilde{g}}^2/\hat{s}}$ is the velocity of the gluino in the partonic center-of-mass frame with $\hat{s} = (p_1+p_2)^2$.

The product of the two color-octet states transforms as $\mathbf{8}\otimes\mathbf{8} = \mathbf{1}\oplus\mathbf{8_S}\oplus\mathbf{8_A}\oplus\mathbf{10}\oplus\overline{\mathbf{10}}\oplus\mathbf{27}$. In the $gg\to\tilde{g}\tilde{g}$ amplitudes, the color basis for these states can be taken as [12];

$$\mathbf{1}: \quad c_1 = \frac{1}{8}\delta^{a_1a_2}\delta^{a_3a_4}, \tag{3.5a}$$

$$\mathbf{8_S}: \quad c_2 = \frac{3}{5}d^{a_1a_2b}d^{a_3a_4b}, \tag{3.5b}$$

$$\mathbf{8_A}: \quad c_3 = \frac{1}{3}f^{a_1a_2b}f^{a_3a_4b}, \tag{3.5c}$$

$$\mathbf{10}\oplus\overline{\mathbf{10}}: \quad c_4 = \frac{1}{2}\left(\delta^{a_1a_3}\delta^{a_2a_4}-\delta^{a_1a_4}\delta^{a_2a_3}\right)-\frac{1}{3}f^{a_1a_2b}f^{a_3a_4b}, \tag{3.5d}$$

$$\mathbf{27}: \quad c_5 = \frac{1}{2}\left(\delta^{a_1a_3}\delta^{a_2a_4}+\delta^{a_1a_4}\delta^{a_2a_3}\right)-\frac{1}{8}\delta^{a_1a_2}\delta^{a_3a_4}-\frac{3}{5}d^{a_1a_2b}d^{a_3a_4b}, \tag{3.5e}$$

where the bases c_1 to c_5 are for $\mathbf{1}$, $\mathbf{8_S}$, $\mathbf{8_A}$, $\mathbf{10}\oplus\overline{\mathbf{10}}$, $\mathbf{27}$, respectively. The color factors in eq. (3.2) are then expressed as

$$\frac{1}{2}\left\{F^{a_1},F^{a_2}\right\}_{a_3a_4} = \frac{1}{2}\left(f^{a_1a_3b}f^{a_2a_4b}+f^{a_1a_4b}f^{a_2a_3b}\right) = 3c_1+\frac{3}{2}c_2-c_5, \tag{3.6}$$

$$\frac{1}{2}\left[F^{a_1},F^{a_2}\right]_{a_3a_4} = \frac{1}{2}\left(f^{a_1a_3b}f^{a_2a_4b}-f^{a_1a_4b}f^{a_2a_3b}\right) = \frac{3}{2}c_3. \tag{3.7}$$

The c_4 term for $\mathbf{10}\oplus\overline{\mathbf{10}}$ state does not appear at the tree-level. Near the threshold, only the color-symmetric part of the amplitude M_{gg} survives, and the anti-symmetric part N_{gg} is suppressed by β. Thus, production cross-section for the color-$\mathbf{8_A}$ state is suppressed by $\mathcal{O}(\beta^2)$ near the threshold. All the other color-states have the same production amplitude at the tree-level, with the normalization constant $(|3c_1|^2, |3/2c_2|^2, |c_5|^2) = (9, 18, 27)$. Therefore, 1/6 of gluino-pair produced near the threshold is in the color-singlet, while 1/3, 1/2 are in the $\mathbf{8_S}$, $\mathbf{27}$ color-states, respectively.

JHEP10(2009)049

3.2 $q\bar{q} \to \tilde{g}\tilde{g}$ process

Next, we examine the $q\bar{q}$ annihilation process. In contrast to the $q\bar{q} \to Q\bar{Q}$ process where only the color-octet state are produced, the color-singlet $\tilde{g}\tilde{g}$ state can also be produced due to the squark-exchange diagrams; see figure 2.

Helicity amplitudes for this process are written as;

$$\mathcal{M}_{q\bar{q}\to\tilde{g}\tilde{g}}(p_k;\lambda_k;i_k,a_k) = g_s^2\left[\frac{1}{2}\{T^{a_3},T^{a_4}\}_{i_1i_2}M_{q\bar{q}}(p_k;\lambda_k)+\frac{1}{2}[T^{a_3},T^{a_4}]_{i_1i_2}N_{q\bar{q}}(p_k;\lambda_k)\right]. \tag{3.8}$$

The color-symmetric amplitudes are

$$M_{q\bar{q}}(p_k;\lambda,-\lambda,\bar{\lambda},\bar{\lambda}) = \bar{\lambda}\frac{4m_{\tilde{g}}}{\sqrt{\hat{s}}}\frac{\beta\cos\theta\sin\theta}{A_\lambda^2-\beta^2\cos^2\theta}, \tag{3.9a}$$

$$M_{q\bar{q}}(p_k;\lambda,-\lambda,\bar{\lambda},-\bar{\lambda}) = -2\beta(1+\lambda\bar{\lambda}\cos\theta)\frac{A_\lambda-\lambda\bar{\lambda}\cos\theta}{A_\lambda^2-\beta^2\cos^2\theta}, \tag{3.9b}$$

and the anti-symmetric ones are

$$N_{q\bar{q}}(p_k;\lambda,-\lambda,\bar{\lambda},\bar{\lambda}) = \bar{\lambda}\frac{4m_{\tilde{g}}}{\sqrt{\hat{s}}}\sin\theta\left[1-\frac{A_\lambda}{A_\lambda^2-\beta^2\cos^2\theta}\right], \tag{3.10a}$$

$$N_{q\bar{q}}(p_k;\lambda,-\lambda,\bar{\lambda},-\bar{\lambda}) = 2\left(\lambda\bar{\lambda}+\cos\theta\right)\left[1-\frac{A_\lambda-\lambda\bar{\lambda}\beta^2\cos\theta}{A_\lambda^2-\beta^2\cos^2\theta}\right]. \tag{3.10b}$$

Here, we define $A_\lambda = 1-2(m_{\tilde{g}}^2-m_{\tilde{q}_\lambda}^2)/\hat{s}$ where $\tilde{q}_+ = \tilde{q}_R$ and $\tilde{q}_- = \tilde{q}_L$. Due to the chirality conservation, amplitudes for $\lambda_1 = \lambda_2$ vanish and only the squark with the chirality of the incoming quark $\lambda = \lambda_1$ contributes. In the threshold limit $\beta \to 0$, the color-symmetric amplitudes behave as $M_{q\bar{q}} \sim \mathcal{O}(\beta)$ and the anti-symmetric ones as $N_{q\bar{q}} \propto (m_{\tilde{g}}^2-m_{\tilde{q}_\lambda}^2)/(m_{\tilde{g}}^2+m_{\tilde{q}_\lambda}^2)$. Note that, the first term in the square bracket in eqs. (3.10) comes from the s-channel gluon exchange diagram, while the other term comes from squark-exchange diagrams. When $A_\lambda = 1$ i.e. when the gluino mass and the squark mass are degenerate, the s-channel diagram and squark-exchange diagrams interfere destructively [9] to make the full amplitudes (3.8) color-symmetric.

The color states of the produced gluino pair are found from

$$\frac{1}{2}\{T^a,T^b\}_{ij} = \frac{1}{2N}\delta^{ab}\delta_{ij}+\frac{1}{2}d^{abc}T^c_{ij}, \tag{3.11a}$$

$$\frac{1}{2}[T^a,T^b]_{ij} = \frac{1}{2}if^{abc}T^c_{ij}. \tag{3.11b}$$

The first term in the right-hand side in eq. (3.11a) represents the color-singlet, and the others are color-octets either symmetric (3.11a) or anti-symmetric (3.11b). Thus, in $q\bar{q}$ annihilation, production of the color-singlet state is suppressed by $\mathcal{O}(\beta^2)$ and the color-octet state ($\mathbf{8_A}$) dominates near the threshold, unless the gluino mass and the squark mass are degenerate.

4 Binding corrections

In this section, we describe the bound-state effects in the gluino-pair production. The partonic cross-section including bound-state correction is expressed as;

$$\hat{\sigma}_i^{(c)}(\hat{s}) = \hat{\sigma}_{i,0}^{(c)}(\hat{s}) \cdot \frac{\mathrm{Im}[G^{(c)}(\vec{0}, E + i\Gamma_{\tilde{g}})]}{\mathrm{Im}[G_0(\vec{0}, E + i\Gamma_{\tilde{g}})]}, \tag{4.1}$$

where $\hat{\sigma}_{i,0}^{(c)}$ is the tree-level cross-section. Here, we specify the color-state of the gluino-pair denoted by c, and i represents the initial partons $i = gg$ or $q\bar{q}$. The Green's function $G^{(c)}$ is obtained by solving the Schödinger equation;

$$\left[(E + i\Gamma_{\tilde{g}}) - \left\{-\frac{\nabla^2}{m_{\tilde{g}}} + V^{(c)}(r)\right\}\right] G^{(c)}(\vec{x}; E + i\Gamma_{\tilde{g}}) = \delta^3(\vec{x}), \tag{4.2}$$

where E is an energy of the gluino-pair measured from their mass threshold. We define it as,

$$E = \begin{cases} M - 2m_{\tilde{g}} & (M < 2m_{\tilde{g}}) \\ m_{\tilde{g}}\,\beta^2 & (M \geq 2m_{\tilde{g}}) \end{cases}, \tag{4.3}$$

where M is the invariant-mass of the gluino-pair. $V^{(c)}(r)$ is QCD potentials between the gluino-pair depending on their colors. G_0 is obtained by taking $V^{(c)} = 0$, which is simply the tree-level Green's function of the gluinos with its finite width.

We use the NLO QCD potential [33];

$$V^{(c)}(r) = C^{(c)} \frac{\alpha_s(\mu_B)_{\overline{\mathrm{MS}}}}{r} \left[1 + \frac{\alpha_s}{\pi}\left\{2\beta_0\left[\ln(\mu_B r) + \gamma_E\right] + a_1\right\} + \mathcal{O}\left(\left(\frac{\alpha_s}{\pi}\right)^2\right)\right] \tag{4.4}$$

where the color-factor $C^{(c)}$ is known [23] to be

$$C^{(c)} = \left\{-C_A, -\frac{1}{2}C_A, -\frac{1}{2}C_A, 0, 1\right\}, \tag{4.5}$$

for $c = \{\mathbf{1}, \mathbf{8_S}, \mathbf{8_A}, \mathbf{10} \oplus \overline{\mathbf{10}}, \mathbf{27}\}$, respectively. Thus, QCD potential for $\mathbf{1}$, $\mathbf{8_S}$ and $\mathbf{8_A}$ color-states is attractive, while that for $\mathbf{27}$ color-state is repulsive. $\gamma_E = 0.5772\ldots$ denotes the Euler constant, and the other constants are;

$$\beta_0 = \frac{11}{3}C_A - \frac{2}{3}n_q, \quad a_1 = \frac{31}{9}C_A - \frac{10}{9}n_q. \tag{4.6}$$

We take the number of light-quark flavor to $n_q = 5$, and the scale μ_B as a half of the inverse Bohr radius of the color-singlet gluinonium, $\mu_B = 1/2r_B = C_A m_{\tilde{g}} \alpha_s(\mu_B)/4$. For example for $m_{\tilde{g}} = 608\,\mathrm{GeV}$, we obtain $\mu_B \simeq 58\,\mathrm{GeV}$ and $\alpha_s(\mu_B) \simeq 0.127$. With this scale choice, the higher-order corrections to the binding energy is small. On the other hand, the magnitude of the Green's function is reduced by several tens percent in an entire range of E, when one includes the NLO correction.

For the attractive force, the gluino-pair forms a bound-state with a definite spin (S) and an orbital angular momenta (L) [23]. Within the MSSM the gluino is a Majorana

JHEP10(2009)049

color	symmetric ($\mathbf{1}$, $\mathbf{8_S}$, $\mathbf{27}$)	anti-symmetric ($\mathbf{8_A}$)
$\tilde{g}\tilde{g}$	${}^1S_0$, ${}^3P_{0,1,2}$, ${}^1D_2$, $\cdots$	${}^3S_1$, ${}^1P_1$, ${}^3D_{1,2,3}$, $\cdots$
$i = gg$	${}^1S_0$, ${}^3P_{0,\ 2}$, ${}^1D_2$, $\cdots$	${}^1P_1$, ${}^3D_{1,\ 3}$, $\cdots$
$i = q\bar{q}$	${}^3P_{\ 1,2}$, $\cdots$	${}^3S_1$, ${}^3D_{1,2,3}$, $\cdots$

Table 1. Summary of gluinonium states, and possible tree-level production from $i = gg$ and $i = q\bar{q}$.

fermion, and the wave-function of the $\tilde{g}\tilde{g}$ state must be anti-symmetric under the exchange of the two gluinos. This leads to the restriction on the spin and orbital angular momenta of the gluinonium, so that the color-symmetric pair in ($\mathbf{1}$, $\mathbf{8_S}$, $\mathbf{27}$) forms only even $L+S$ states, while the color-antisymmetric pair ($\mathbf{8_A}$) forms only odd $L+S$ states. Possible bound-states for each color-state are summarized in table 1. We also list the non-zero components in the tree-level amplitude for each process. Blank states in $i = gg$ and $i = q\bar{q}$ rows are missing at the tree-level. For example, due to the Yang's theorem, color-symmetric $J = 1$ states are forbidden in gluon-fusion process. Likewise, $S = 0$ or $J = 0$ states are forbidden in $i = q\bar{q}$, due to the chirality conservation.

For the repulsive force, the gluino-pair does not form a bound-state, but the Green's function formula is still useful for summing over Coulombic corrections.

In our analysis, we include only the S-wave Green's function. The other states are left free, since they are not affected significantly by the binding effects. The extraction of the certain partial-wave amplitude is straightforward from the helicity amplitudes given in the previous section.

The $\tilde{g}\tilde{g}$ invariant-mass distribution in the hadronic collisions is given as [17, 18];

$$\frac{d\sigma}{dM^2} = \sum_{i,c} \hat{\sigma}_i^{(c)}(M^2) \cdot K_i^{(c)} \int_\tau^1 \frac{dz}{z} F_i^{(c)}(z) \frac{d\mathcal{L}_i}{d\tau}\left(\frac{\tau}{z}\right), \tag{4.7}$$

where $\tau = M^2/s$. The partonic luminosity is defined by

$$\frac{d\mathcal{L}_i}{d\tau}(\tau;\mu_F) = \sum_{\{a,b\}} \int dx_1 \int dx_2 f_a(x_1,\mu_F) f_b(x_2,\mu_F) \delta(\tau - x_1 x_2), \tag{4.8}$$

where the summation is over $\{a,b\} = \{g,g\}$ for $i = gg$, and $\{a,b\} = \{q,\bar{q}\}, \{\bar{q},q\}$ with $q = u,d,s,c,b$ for $i = q\bar{q}$. We use 5-flavor parton distribution functions, and the 5-flavor strong coupling constant even for $\mu > m_t$.

The convolution formula in eq. (4.7) is based on an assumption of the factorization of the soft/collinear gluon emission and the Coulomb corrections.[2] Thus, the soft/collinear gluon emission is described by the ISR (initial-state radiation) functions $F_i^{(c)}$, and the Coulomb corrections are included in the partonic cross-section $\hat{\sigma}_i^{(c)}$, as in eq. (4.1). $K_i^{(c)}$ represents the hard-vertex correction, which is a process-dependent constant.

In this section, we neglect the ISR effect for simplicity, and set $F_i^{(c)}(z) = \delta(1-z)$ with $K_i^{(c)} = 1$. The effect is discussed in the next section.

[2]Recent paper by M. Beneke, P. Falgari and C. Schwinn shows the factorization property of the Coulomb-gluon and the soft-gluon [34].

JHEP10(2009)049

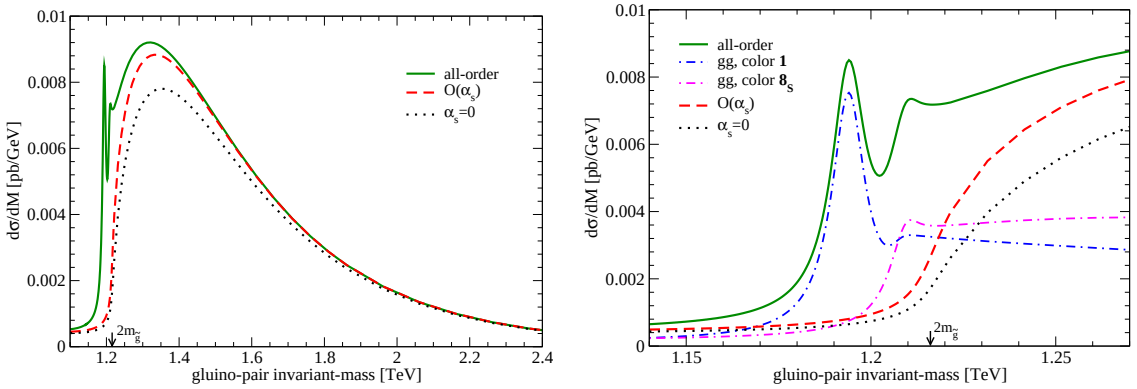

Figure 3. $\tilde{g}\tilde{g}$ invariant-mass distribution at the LHC, for $m_{\tilde{g}} = 608\,\mathrm{GeV}$ and $\Gamma_{\tilde{g}} = 5.5\,\mathrm{GeV}$ (SPS1a). Result in the Born level (dotted), $\mathcal{O}(\alpha_s)$ Coulomb correction (dashed), and the all-order Coulomb correction (solid) are plotted. Right figure is the same, but enlarged for the threshold region. All-order Coulomb correction for individual **1** and $\mathbf{8_S}$ color-states in the gluon-fusion process are also plotted in dot-dashed lines.

In the left figure in figure 3, we show the invariant-mass distribution of the gluino-pair including bound-state corrections, for the LHC with $\sqrt{s} = 14\,\mathrm{TeV}$. The results are given for $m_{\tilde{g}} = 608\,\mathrm{GeV}$, *a la* SPS1a [35], and for $\Gamma_{\tilde{g}} = 5.5\,\mathrm{GeV}$ for $m_{\tilde{q}} = 547\,\mathrm{GeV}$. We use the CTEQ6L PDF parameterization [36], and set scales as $\mu_R = \mu_F = m_{\tilde{g}}$. Predictions in Born-level, including $\mathcal{O}(\alpha_s)$ Coulomb correction, and all-order Coulomb correction are plotted in dotted, dashed and solid lines, respectively. Compared to the Born-level result, the $\mathcal{O}(\alpha_s)$ correction as well as the all-order Coulomb corrections bring large enhancement near the mass threshold ($M \simeq 2m_{\tilde{g}}$). Moreover, the distribution for the all-order correction indicates the resonance peaks below the threshold. Due to the binding correction and the finite-width effect, the gluino-pair invariant-mass distribution arises rapidly below the mass threshold. Thus the effective pair-production threshold is not at $2m_{\tilde{g}}$ but at $M \simeq 2m_{\tilde{g}} - 30\,\mathrm{GeV}$. The order of the deviation is about the binding-energy of the ${}^1S_0(\mathbf{1})$ state, thus $\mathcal{O}(m_{\tilde{g}}\alpha_s^2)$. On the other hand, the enhancement disappears in the high invariant-mass region.

The all-order Coulomb correction enhance the total cross-section by about 15% from the cross-section in Born level, where a substantial portion from below the threshold region contributes. We discuss this result in more detail below.

The right figure in figure 3 is the same, but enlarged on the threshold region. For the all-order correction, individual contributions of the color **1**, $\mathbf{8_S}$ states are also plotted. But those for other color-states, $\mathbf{8_A}$, **27** which have no enhancement near the threshold are not shown. $q\bar{q}$ annihilation process is negligible in this case. In the all-order distribution, two resonance peaks can be found at $E \simeq -22\,\mathrm{GeV}$ and $E \simeq -7\,\mathrm{GeV}$. The first peak corresponds to the ground state of the color-singlet ${}^1S_0$ resonance, and the second peak consists of the second excitation of the ${}^1S_0(\mathbf{1})$ resonance and the ground state of the ${}^1S_0(\mathbf{8_S})$ resonance.

Figure 4 is also the invariant-mass distributions at the very threshold region, considering a variety of the gluino decay width. Results for $m_{\tilde{g}} = 608\,\mathrm{GeV}$, for $\Gamma_{\tilde{g}} = 20\,\mathrm{GeV}$, $5.5\,\mathrm{GeV}$, $1.5\,\mathrm{GeV}$ and $0.5\,\mathrm{GeV}$ are plotted in the dotted, dot-dashed, dashed and solid lines, respectively.

JHEP10(2009)049

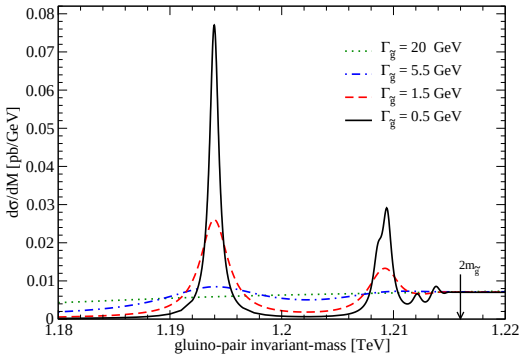

Figure 4. Invariant-mass distributions at the threshold region, at the LHC, $\sqrt{s} = 14\,\text{TeV}$. Results including the all-order Coulomb correction, as well as no Coulomb correction are plotted for $m_{\tilde{g}} = 608\,\text{GeV}$, for $\Gamma_{\tilde{g}} = 20\,\text{GeV}$ (dotted), $5.5\,\text{GeV}$ (dot-dashed) $1.5\,\text{GeV}$ (dashed) and $0.5\,\text{GeV}$ (solid).

According to figure 1, $\Gamma_{\tilde{g}} = 20\,\text{GeV}$ is the same order as the gluinonium binding energy $|E_B| \simeq 22\,\text{GeV}$ for $m_{\tilde{g}} = 608\,\text{GeV}$. Thus it corresponds to the region A according to the classification defined in section 2. In this case, the invariant-mass distribution shows no resonance peaks, but a gradual slope until rather below the threshold. This is due to the finite width effect, giving the production probability of the events with a off-shell gluino. The Coulomb corrections act to enhance the production ratio at the threshold region. Next, $\Gamma_{\tilde{g}} = 5.5\,\text{GeV}$ is the same value as used in figure 3 which corresponds to the region B. This case, the distribution shows a broad resonance at $E \simeq -22\,\text{GeV}$, corresponding to the ground ${}^1S_0(\mathbf{1})$ gluinonium. The resonance for the ground ${}^1S_0(\mathbf{8_S})$ gluinonium at $E \simeq -7\,\text{GeV}$ is barely seen. In the distribution for $\Gamma_{\tilde{g}} = 1.5\,\text{GeV}$ (region C), the two separated resonances for the ground ${}^1S_0(\mathbf{1})$ and ${}^1S_0(\mathbf{8_S})$ gluinoniums can be seen. Finally, for $\Gamma_{\tilde{g}} = 0.5\,\text{GeV}$ (region D), several resonances can be found in $M < 2m_{\tilde{g}}$. Actually, the first peak for the ground ${}^1S_0(\mathbf{1})$ resonance is quite sharp. The second peak at $E \simeq -7\,\text{GeV}$ which consists of the ground ${}^1S_0(\mathbf{8_S})$ gluinonium and the second excited ${}^1S_0(\mathbf{1})$ gluinonium is also clearly seen.

As mentioned in section 2, for the regions C and D, the partial decay width of the gluinonium annihilation into gluons can not be negligible. For $m_{\tilde{g}} = 608\,\text{GeV}$, the two gluon decay-width of the ${}^1S_0(\mathbf{1})$ gluinonium is about $\Gamma_{gg}[{}^1S_0(\mathbf{1})] \simeq 0.75\,\text{GeV}$, see eq. (2.3) and figure 1. Note that the gluinoniums have partial decay width $2\Gamma_{\tilde{g}}$, due to the decay width of the constituent gluinos. Thus, the branching ratio to the "hidden" gluino decay may be estimated by $B((\tilde{g}\tilde{g}) \to gg) = \Gamma_{gg}/(2\Gamma_{\tilde{g}} + \Gamma_{gg})$. Using this estimation, about 20% (40%) of the resonance events for $\Gamma_{\tilde{g}} = 1.5\,\text{GeV}$ (0.5 GeV) in figure 4 would decay into jets. Therefore, only 80% (60%) of the resonance events would leave detectable signals of the gluinos at hadron colliders.

A correction to the total cross-section is also an important consequence of the inclusion of the binding corrections. Above the threshold, the all-order summation of the Coulomb corrections gives the Sommerfeld factor. It enhances the total cross-section from the Born-level results by 10% to 20% for $m_{\tilde{g}} = 200\,\text{GeV}$ to 2 TeV, almost independent of the gluino decay-width. This result is rather smaller than that in ref. [14], due to the NLO correction to the QCD potential which reduces the magnitude of the Green's function even for $E \gtrsim 0$.

JHEP10(2009)049

$m_{\tilde{g}}$	A: $\Gamma_{\tilde{g}} = E_B$	B: $\Gamma_{\tilde{g}} = E_B/2$	C: $\Gamma_{\tilde{g}} = 2\Gamma_{gg}$	D: $\Gamma_{\tilde{g}} = \Gamma_{gg}/2$
200 [GeV]	7.5 [4.5]	5.0 [1.8]	4.0 [0.3]	3.9 [0.1]
400 [GeV]	7.1 [4.2]	4.8 [1.7]	3.8 [0.2]	3.8 [0.1]
600 [GeV]	7.2 [4.2]	5.0 [1.7]	3.9 [0.2]	4.2 [0.0]
1 [TeV]	7.9 [4.6]	5.5 [1.8]	4.3 [0.2]	4.4 [0.0]
1.5 [TeV]	9.2 [5.3]	6.3 [2.1]	5.0 [0.2]	5.1 [0.0]
2 [TeV]	10.7 [6.3]	7.4 [2.5]	5.9 [0.2]	5.9 [0.0]

Table 2. Table of a proportion of the cross section in $M < 2m_{\tilde{g}}$ to the total cross-section (%), at the LHC with $\sqrt{s} = 14\,\text{TeV}$. The same ratio but without the binding correction are also listed in the squark bracket.

In addition, there comes a substantial portion to the total cross section from the $M < 2m_{\tilde{g}}$ region. The cross section in this region emerges by (1) the smearing effect due to the finite width of the gluino, and (2) the bound-state contributions. The former is proportional to $\Gamma_{\tilde{g}}$, while the later is almost independent of $\Gamma_{\tilde{g}}$.

In table 2, we calculate the proportion of the cross section in $M < 2m_{\tilde{g}}$ to the total cross-section. We define the total cross-section by integrating the differential cross-section over the invariant-mass from $M = 2m_{\tilde{g}} + E_B[^1S_0(\mathbf{1})] - 3\Gamma_{\tilde{g}}$ to $\sqrt{s}$, where $E_B[^1S_0(\mathbf{1})]$ is the binding energy of the $^1S_0(\mathbf{1})$ gluinonium. $\Gamma_{\tilde{g}} = E_B[^1S_0(\mathbf{1})]$, $E_B[^1S_0(\mathbf{1})]/2$, $2\Gamma_{gg}[^1S_0(\mathbf{1})]$ and $\Gamma_{gg}[^1S_0(\mathbf{1})]/2$, for $m_{\tilde{g}} = 200\,\text{GeV}$ to $2\,\text{TeV}$ are examined. The four patterns of $\Gamma_{\tilde{g}}$ represent typical values in the regions A to D. In the square brackets are the same ratio but without the binding correction, thus these illustrate only the finite-width effect of the gluino.

For $\Gamma_{\tilde{g}} = E_B$ (region A), the ratio grows from 8% for smaller $m_{\tilde{g}}$ to 11% for larger $m_{\tilde{g}}$, where a more than half of the contribution comes from the smearing effect due to the large decay width. The smearing effect decreases with $\Gamma_{\tilde{g}}$, and is negligible for the regions C and D. Then the bound-state effect which tends from 4% to 6% dominates the ratio. Basically, the ratio grows with $m_{\tilde{g}}$. This is because, for larger $m_{\tilde{g}}$, the gluon luminosity becomes more steep in M, thus the cross section in lower invariant-mass region is more significant.

5 ISR corrections

In this section, we discuss the effects of the ISR and the hard correction, which are the remaining major corrections in QCD. We treat the ISR function to $\mathcal{O}(\alpha_s)$ in a soft approximation, as in ref. [17]. The ISR function defined in eq. (4.7) is written up to NLO as;

$$F_i^{(c)}(z;\mu_F) = \delta(1-z) + \frac{\alpha_s(\mu_F)}{\pi}\left[f_i^{(c)}\left(z,\frac{\mu_F}{m_{\tilde{g}}}\right) + k_i^{(c)}\left(\frac{\mu_F}{m_{\tilde{g}}}\right)\delta(1-z)\right], \tag{5.1}$$

with

$$f_i^{(c)}\left(z,\frac{\mu_F}{2m_{\tilde{g}}}\right) = 4A_i\left[\left(\frac{\ln(1-z)}{1-z}\right)_+ - \left(\frac{1}{1-z}\right)_+ \ln\left(\frac{\mu_F}{2m_{\tilde{g}}}\right)\right] + D_c\left(\frac{1}{1-z}\right)_+. \tag{5.2}$$

and

$$k_i^{(c)}\left(\frac{\mu_F}{m_{\tilde{g}}}\right) = 2B_i \ln\left(\frac{\mu_F}{2m_{\tilde{g}}}\right). \tag{5.3}$$

The constants are given as [12];

$$\begin{aligned} &A_g = C_A, \quad A_q = C_F, \qquad B_g = -\frac{\beta_0}{2}, \quad B_q = -\frac{3}{2}C_F, \\ &D_{\mathbf{1}} = 0, \quad D_{\mathbf{8_S}} = -3, \quad D_{\mathbf{8_A}} = -3, \quad D_{\mathbf{27}} = -8. \end{aligned} \tag{5.4}$$

The hard-vertex factor is obtained by matching with the full $\mathcal{O}(\alpha_s)$ correction. However, to our knowledge, $\mathcal{O}(\alpha_s)$ correction to the gluino-pair production has been calculated numerically and only for the color-summed cross-section in ref. [9]. Accordingly, we cannot fixed the color-dependent factors, but only the color-averaged one. We parametrize the hard-vertex factors as

$$K_i^{(c)}(\mu_R) = 1 + \frac{\alpha_s(\mu_R)}{\pi} h_i^{(c)}\left(\frac{\mu_R}{m_{\tilde{g}}}\right), \tag{5.5}$$

with

$$h_i\left(\frac{\mu_R}{m_{\tilde{g}}}\right) = \bar{h}_i + \beta_0 \ln\left(\frac{\mu_R}{2m_{\tilde{g}}}\right). \tag{5.6}$$

Extracting from the graphs in the figure 9 (a) and (b) in ref. [9] or using ref. [10], we find

$$\bar{h}_g = -0.26, \tag{5.7}$$

$$\bar{h}_q = 1.5, \tag{5.8}$$

where the later is obtained for $m_{\tilde{q}}/m_{\tilde{g}} = 1.4$, and we neglect the mass-ratio dependence. There is also an ambiguity in separating the non-logarithmic part in $k_i^{(c)}$ and $h_i^{(c)}$. We take a scheme such that the non-logarithmic part in $k_i^{(c)}$ is zero.

Now, we examine the ISR effect to the differential cross section at the bound-state region. We calculate the ratio of $d\sigma/dM$ at $M = 2m_{\tilde{g}} + E_B$ including the ISR to that without the ISR, $K \equiv \sigma_{\rm ISR}/\sigma_{\rm No\,ISR}$, where $d\sigma/dM$ with the ISR are evaluated using the CTEQ6M PDFs with $\mu = m_{\tilde{g}}$.

We also examine the ambiguity by the scale choice of μ. We find the maximum and the minimum of $d\sigma/dM$ at $M = 2m_{\tilde{g}} + E_B$ during the range from $\mu = m_{\tilde{g}}$ to $2m_{\tilde{g}}$, and define the uncertainty for the cross sections without and with the ISR as

$$\delta_{\{\rm No\,ISR,\,ISR\}} \equiv \frac{\sigma_{\rm max} - \sigma_{\rm min}}{\sigma(\mu = m_{\tilde{g}})}. \tag{5.9}$$

In table 3, we list the ratio K and the scale uncertainties δ for the cross-section without and with the ISR. In the calculation, the decay width is set to $\Gamma_{\tilde{g}} = E_B/2$, however the width dependence is small. The ratio K is 1.2 for $m_{\tilde{g}} = 200\,\text{GeV}$ and increases with $m_{\tilde{g}}$ to 2.8 for $m_{\tilde{g}} = 2\,\text{TeV}$, due to the terms including the plus distribution in $F_i^{(c)}$, which take large values when $\hat{s}$ is close to M^2. The scale uncertainty of the cross section without the ISR is 21-25%, however that with the ISR is remarkably reduced to a few percent.

JHEP10(2009)049

$m_{\tilde{g}}$	K	$\delta_{\text{No ISR}}$	δ_{ISR}
200 [GeV]	1.17	0.21	0.05
400 [GeV]	1.36	0.22	0.02
600 [GeV]	1.52	0.23	0.01
1 [TeV]	1.82	0.24	0.02
1.5 [TeV]	2.25	0.25	0.03
2 [TeV]	2.78	0.25	0.05

Table 3. Table of the ratio of the differential cross section $d\sigma/dM$ at $M = 2m_{\tilde{g}} + E_B$ with the ISR to that without the ISR, as well as the scale uncertainties $\delta\sigma/\sigma$.

In the invariant-mass distribution, the size of the ISR correction is not actually a constant, but moderately increase with M. As the result, the proportion of the cross section in $M < 2m_{\tilde{g}}$ to the total cross section shown in table 2 is slightly reduced.

We note several remarks on the ISR. First, it is pointed out in the top-quark production [18] that the emission of the non-collinear gluon can give the same-order correction. This can be implemented into our analysis by utilizing the NLO calculation of the gluinonium production which has not been available yet. Moreover, the color-dependence of the hard-vertex factor is neglected in our analysis, which is also resolved by the above calculation or the NLO calculation of the gluino-pair production with an explicit color projection. Due to the lack of them, our results have ambiguity in the overall magnitude of the ISR correction. However, we expect that these effects would not considerably deform the invariant-mass distribution.

6 Summary

In this paper, we study the bound-state corrections in the gluino-pair production at hadron colliders. We perform the all-order summation of the Coulomb corrections using the Green's function formalism, and find sizable corrections in the gluino-pair invariant-mass distribution as well as in the total cross-section.

The consequence of the bound-state correction crucially depends on the decay width of the gluino. When $m_{\tilde{g}} > m_{\tilde{q}}$, the gluino decay-width is typically between a few and a few hundred GeV; see figure 1. In this case, the invariant-mass distribution below and near the mass threshold region receive a large enhancement, due to the formation of the gluinonium bound-states. We show that the gluino-pair production cross section below the threshold ($M < 2m_{\tilde{g}}$) grows from 4% to 6% of the total cross section due to the bound-states formation, when the gluino mass increases from 200 GeV to 2 TeV. For the large $\Gamma_{\tilde{g}}$ case, although the resonance peaks are smeared-out, the ratio grows to 8% to 11% due to the smearing effect. When $\Gamma_{\tilde{g}}$ is significantly smaller than the binding energy of the gluinoniums, which grows from ~ 10 GeV for $m_{\tilde{g}} \simeq 200$ GeV to ~ 50 GeV for $m_{\tilde{g}} = 2$ TeV (see figure 1), one or two resonance peaks arise in the invariant-mass distribution. Although the study of the observable signals of the gluino-pair production, such as the missing p_T and various kinematical observables, is beyond the scope of this report, those events below the threshold should be taken into account in the determination of the gluino mass.

JHEP10(2009)049

On the other hand, when $m_{\tilde{g}} < m_{\tilde{q}}$, the gluino decay-width is quite tiny; see figure 1. In this case, the gluinonium spectra are very sharp and more than two resonance peaks are expected (see figure 4). However, the produced gluinonium resonances would decay mainly into gluon jets and they may escape detections at hadron collider experiments.

Acknowledgments

We wish to send special thanks to Y. Sumino for valuable comments and discussions. We also thank organizers of an LHC-focus week meeting at the IPMU (Institute for the Physics and Mathematics of the Universe) in March 2009, where we enjoyed stimulating discussions and received useful comments from the participants. This work is supported in part by the Grant-in-Aid for scientific research (No. 20340064).

References

[1] ATLAS collaboration, A. Airapetian et al., *ATLAS detector and physics performance: Technical Design Report, 2*, ATLAS-TDR-015, CERN-LHCC-99-015.

[2] CMS collaboration, G.L. Bayatian et al., *CMS technical design report, volume II: Physics performance*, CERN-LHCC-2006-021, *J. Phys.* **G 34** (2007) 995 [SPIRES].

[3] D0 collaboration, V.M. Abazov et al., *Search for squarks and gluinos in events with jets and missing transverse energy using 2.1 fb^{-1} of $p\bar{p}$ collision data at $\sqrt{s} = 1.96$ TeV*, *Phys. Lett.* **B 660** (2008) 449 [arXiv:0712.3805] [SPIRES].

[4] CDF collaboration, T. Aaltonen et al., *Inclusive Search for Squark and Gluino Production in $p\bar{p}$ Collisions at $\sqrt{s} = 1.96$ TeV*, *Phys. Rev. Lett.* **102** (2009) 121801 [arXiv:0811.2512] [SPIRES].

[5] Particle Data Group collaboration, C. Amsler et al., *Review of particle physics*, *Phys. Lett.* **B 667** (2008) 1 [SPIRES].

[6] P.R. Harrison and C.H. Llewellyn Smith, *Hadroproduction of Supersymmetric Particles*, *Nucl. Phys.* **B 213** (1983) 223 [*Erratum ibid.* **B 223** (1983) 542] [SPIRES].

[7] S. Dawson, E. Eichten and C. Quigg, *Search for Supersymmetric Particles in Hadron - Hadron Collisions*, *Phys. Rev.* **D 31** (1985) 1581 [SPIRES].

[8] H.E. Haber and G.L. Kane, *The Search for Supersymmetry: Probing Physics Beyond the Standard Model*, *Phys. Rept.* **117** (1985) 75 [SPIRES].

[9] W. Beenakker, R. Hopker, M. Spira and P.M. Zerwas, *Squark and gluino production at hadron colliders*, *Nucl. Phys.* **B 492** (1997) 51 [hep-ph/9610490] [SPIRES].

[10] W. Beenakker, R. Hopker and M. Spira, *PROSPINO: A program for the PROduction of Supersymmetric Particles In Next-to-leading Order QCD*, hep-ph/9611232 [SPIRES].

[11] W. Beenakker, M. Krämer, T. Plehn, M. Spira and P.M. Zerwas, *Stop production at hadron colliders*, *Nucl. Phys.* **B 515** (1998) 3 [hep-ph/9710451] [SPIRES].

[12] A. Kulesza and L. Motyka, *Threshold resummation for squark-antisquark and gluino- pair production at the LHC*, *Phys. Rev. Lett.* **102** (2009) 111802 [arXiv:0807.2405] [SPIRES].

[13] U. Langenfeld and S.-O. Moch, *Higher-order soft corrections to squark hadro- production*, arXiv:0901.0802 [SPIRES].

JHEP10(2009)049

[14] A. Kulesza and L. Motyka, *Soft gluon resummation for the production of gluino-gluino and squark-antisquark pairs at the LHC*, arXiv:0905.4749 [SPIRES].

[15] V.S. Fadin, V.A. Khoze and T. Sjöstrand, *On the threshold behavior of heavy top production*, *Z. Phys.* **C 48** (1990) 613 [SPIRES].

[16] S. Catani, M.L. Mangano, P. Nason and L. Trentadue, *The Top cross-section in hadronic collisions*, *Phys. Lett.* **B 378** (1996) 329 [hep-ph/9602208] [SPIRES].

[17] K. Hagiwara, Y. Sumino and H. Yokoya, *Bound-state Effects on Top Quark Production at Hadron Colliders*, *Phys. Lett.* **B 666** (2008) 71 [arXiv:0804.1014] [SPIRES].

[18] Y. Kiyo, J.H. Kuhn, S. Moch, M. Steinhauser and P. Uwer, *Top-quark pair production near threshold at LHC*, *Eur. Phys. J.* **C 60** (2009) 375 [arXiv:0812.0919] [SPIRES].

[19] I.I.Y. Bigi, V.S. Fadin and V.A. Khoze, *Stop near threshold*, *Nucl. Phys.* **B 377** (1992) 461 [SPIRES].

[20] D.V. Nanopoulos, S. Ono and T. Yanagida, *How would the world look if there were supersymmetric particles?*, *Phys. Lett.* **B 137** (1984) 363 [SPIRES].

[21] J.H. Kuhn and S. Ono, *Production and decay of gluino-gluino bound states*, *Phys. Lett.* **B 142** (1984) 436 [SPIRES].

[22] W.-Y. Keung and A. Khare, *Two-gluino bound states*, *Phys. Rev.* **D 29** (1984) 2657 [SPIRES].

[23] J.T. Goldman and H. Haber, *Gluinonium: The Hydrogen Atom of Supersymmetry*, *Physica* **D 15** (1985) 181 [SPIRES].

[24] V.G. Kartvelishvili, A.V. Tkabladze and E.G. Chikovani, *Octet bound states of the gluinos*, *Z. Phys.* **C 43** (1989) 509 [SPIRES].

[25] K. Hagiwara, K. Kato, A.D. Martin and C.K. Ng, *Properties of heavy quarkonia and related states*, *Nucl. Phys.* **B 344** (1990) 1 [SPIRES].

[26] E. Chikovani, V. Kartvelishvili, R. Shanidze and G. Shaw, *Bound states of two gluinos at the Tevatron and CERN LHC*, *Phys. Rev.* **D 53** (1996) 6653 [hep-ph/9602249] [SPIRES].

[27] K. Cheung and W.-Y. Keung, *Split supersymmetry, stable gluino and gluinonium*, *Phys. Rev.* **D 71** (2005) 015015 [hep-ph/0408335] [SPIRES].

[28] V.A. Khoze, A.D. Martin and M.G. Ryskin, *Prospects for new physics observations in diffractive processes at the LHC and Tevatron*, *Eur. Phys. J.* **C 23** (2002) 311 [hep-ph/0111078] [SPIRES].

[29] V.S. Fadin and V.A. Khoze, *Threshold Behavior of Heavy Top Production in e^+e^- Collisions*, *JETP Lett.* **46** (1987) 525 [*Pisma Zh. Eksp. Teor. Fiz.* **46** (1987) 417] [SPIRES].

[30] V.S. Fadin and V.A. Khoze, *Production of a pair of heavy quarks in e^+e^- annihilation in the threshold region*, *Sov. J. Nucl. Phys.* **48** (1988) 309 [*Yad. Fiz.* **48** (1988) 487] [SPIRES].

[31] M. Drees, R. Godbole and P. Roy, *Theory and phenomenology of sparticles: An account of four-dimensional $N = 1$ supersymmetry in high energy physics*, World Scientific, Hackensack, U.S.A. (2004), and references therein.

[32] R.M. Barnett, J.F. Gunion and H.E. Haber, *Gluino decay patterns and signatures*, *Phys. Rev.* **D 37** (1988) 1892 [SPIRES].

[33] B.A. Kniehl, A.A. Penin, Y. Schroder, V.A. Smirnov and M. Steinhauser, *Two-loop static QCD potential for general colour state*, *Phys. Lett.* **B 607** (2005) 96 [hep-ph/0412083] [SPIRES].

JHEP10(2009)049

[34] M. Beneke, P. Falgari and C. Schwinn, *Soft radiation in heavy-particle pair production: all-order colour structure and two-loop anomalous dimension*, arXiv:0907.1443 [SPIRES].

[35] B.C. Allanach et al., *The Snowmass points and slopes: Benchmarks for SUSY searches*, in *Proceedings of the APS/DPF/DPB Summer Study on the Future of Particle Physics (Snowmass 2001)*, Snowmass, Colorado, U.S.A., June 30 – July 21 2001, N. Graf ed., *Eur. Phys. J.* **C 25** (2002) 113 [hep-ph/0202233] [SPIRES].

[36] J. Pumplin et al., *New generation of parton distributions with uncertainties from global QCD analysis*, *JHEP* **07** (2002) 012 [hep-ph/0201195] [SPIRES].

JHEP10(2009)049